

Modelling of a PMSG based wind turbine system with diode rectifier-based generator side converter

M.Gannoun*[†], J. Arbi-Ziani*[†], M.W. Naouar *[†]

*Université de Tunis El Manar, Ecole Nationale d'Ingénieurs de Tunis, LR11ES15 Laboratoire de Systèmes Electriques, 1002, Tunis, Tunisia

(marwa.gannoun@enit.utm.tn, jihen.alarbi@enit.utm.tn, wissem.naouar@enit.utm.tn)

†

Corresponding Author; M. GANNOUN, Université de Tunis El Manar, Ecole Nationale d'Ingénieurs de Tunis, LR11ES15 Laboratoire de Systèmes Electriques, 1002, Tunis, Tunisia, Tel: +216 55 63 71 92.

Received: 10.05.2022 Accepted:08.06.2022

Abstract- Despite the fact that several research works have been carried out on wind-based distribution generation systems, some niche applications continue to need more research works and additional investigations. Among them, we can quote small power wind turbine systems. These systems are generally assisted by Permanent Magnet Synchronous Generators (PMSG). This is mainly due to the robustness and high-cost effectiveness of PMSGs. Two topologies are commonly used to separate the grid and the PMSG. The first topology is the most used one and is associated to a back-to-back power converter. For the second topology is assisted by a generator side converter that includes a three-phase diode rectifier, an unregulated DC-link, and a boost converter. As for the grid side converter of the second structure, it is based on a three-phase inverter and is connected to the generator side converter by a controlled DC-link. In literature, the second topology, especially its generator side converter, is modeled by linearized and average dynamic models. As a result, it is complicated to develop accurate regulators for small wind turbine systems based on a PMSG with the above mentioned second topology. This paper therefore presents a precise method for an accurate time-continuous model for a small wind turbine system assisted by a PMSG and with a generator side converter based on a three-phase diode rectifier, an unregulated DC-link, and a boost converter. This proposed model is developed under Matlab-Simulink and validated through several simulation tests.

Keywords PMSG, Small Wind Turbine System, Time-continuous model.

1. Introduction

Over the recent decades, the use of wind turbine generators in modern energy production has significantly increased. [1-3] Further, in the recent years, among Renewable Energy Sources (RESs) there has been a particular interest in the use of Wind Turbine Systems (WTSs) in small energy solutions. Small power wind turbine systems were firstly dominated by asynchronous generators. More recently, PMSGs have become the most attractive choice for small power wind turbine systems due to the many advantages they offer. The PMSG does not require external excitation current. Therefore, it can be connected to the turbine in a direct way without the addition of a gearbox. Also, it can operate at low speed and again reduce weight, costs, losses, and maintenance requirements. [4-8]

In the literature, there are several publications that are interested on the modeling of small power wind turbine systems, to characterize their dynamic response according to different operating conditions. [9-11]. There are two main topologies for PMSG associated to small wind turbine sources. The generator side power converter of the first structure is assisted by a three-phase voltage source converter (Fig.1.a). As regards the second topology, its generator side power converter consists of a three-phase diode rectifier, an uncontrolled DC-link, and a boost converter (Fig.1.b). Both topologies use the same grid side converter, which is associated to a three-phase VSC. The first topology requires

a more complicated control system and has higher cost. However, it ensures better control performances especially for the generator side control. The second topology is more reliable with lower cost [12-13]. Its control is very simple with a reduced number of sensors. Currently, the first topology is widely studied, and the related models are accurately defined. However, the second topology needs to be studied in more detail [14-15]. Also, it is important to note that many papers working on wind energy conversion systems. And most of this work deals with high power wind systems.

There is a lack of work on low power wind systems based on PMSG. As mentioned earlier, the structure-based on the topology (PMSG + three-phase diode rectifier +uncontrolled DC-link +Boost converter + regulated DC-link +inverter +three-phase inductive filter) still needs analytic work because the models made to deal with same systems are based on linearized models or average dynamic models. These models are still not accurate and weak. Therefore, the added value of this work is to represent an accurate time-continuous model that will allow to go further in the development of robust and accurate control structures devoted to low power PMSG-based wind turbine systems assisted by a three-phase diode rectifier-based generator side converter.

So, in this work, we will present a useful model for a PMSG assisted to wind turbine source, which is log on to the grid through the second topology depicted on Fig.1. b. Here, it should be noted that, comparing the first topology with the

second structure, the wind power system studied in this work has the following advantages: low converter complexity and high converter reliability [16]. Also, the second topology is widely used for small power wind turbine systems.

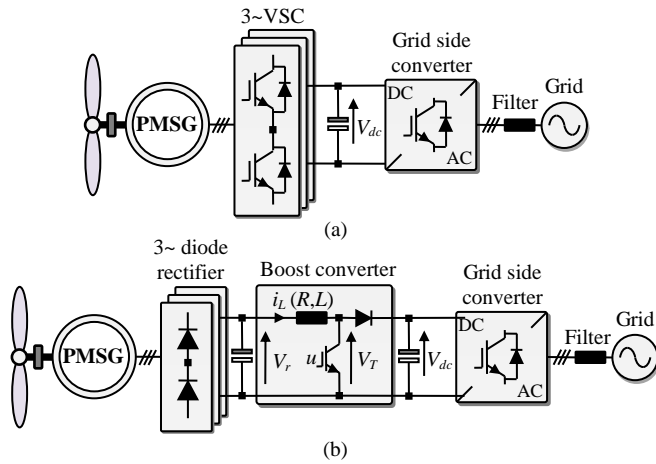


Fig.1. Commonly used topologies for PMSG assisted by wind turbine sources (a) first topology (b) second topology

According to Fig.1.b, the considered PMSG-based wind turbine system includes two power conversion steps. The generator side power converter is composed of a diode rectifier and a boost converter, which are linked through an uncontrolled DC-link. As regards the grid side converter, it is based on a three-phase VSI inverter, which is connected to the grid through an inductive filter. A controlled DC-link interfaces between the AC-DC and the DC-AC conversion stages. The addition of the regulated DC link is to prevent any interaction between the two power conversion parts and to decouple the control of the injected power on the AC side from the power generated by the machine [15]. An accurate model for the two conversion stages will be presented along this work.

The paper is structured as follows: the second section presents the aerodynamic model and the PMSG model. Section 3 presents the model of machine side converter (the AC-DC power converter model). Section 4 presents the model of the grid side converter (the model of the controlled DC-link, the model of the DC-AC converter and the model of the filter). Then, in section 5, the overall system is simulated under Matlab-Simulink. Section 6 summarises the main conclusions of this work.

2. Wind turbine with PMSG model

A. Aerodynamic Model

The rotor blades of the turbine convert the kinetic energy into mechanical energy. The PMSG, as an electrical generator, converts the mechanical energy into electrical energy. The wind turbines generally used for Wind Energy Conversion Systems (WECS) are vertical axis wind turbines (VAWT) or horizontal axis wind turbines (HAWT). HAWTs have the following advantages over VAWTs.

- No need for an initial starting torque.

- It always captures efficient energy from the wind during the entire rotation because the rotation of the blades is perpendicular to the wind.

According to [13], the maximum power value that can be obtained from kinetic power applied to the wind turbine is given by (1).

$$P_{Wind} = \frac{1}{2} \rho A V_{\omega}^3 \quad (1)$$

Where V_{ω} (m/s) is wind velocity, ρ represents the density of air (typically 1.225 kg/m³) and A (m²) is the area swept by the rotor blades.

Hence the output aerodynamic power is provided by:

$$P_{Turbine} = P_{Wind} C_p = \frac{1}{2} \rho A V_{\omega}^3 C_p \quad (2)$$

where C_p is the power coefficient. It represents the ratio of turbine power to the extracted wind power.

The wind turbine mechanical torque output T_m is equal to [17]

$$T_m = \frac{\rho A V_{\omega}^3 C_p(\lambda, \beta)}{2 \omega_m} \quad (3)$$

λ is the tip speed ratio and ω_m (rad/s) is the rotor mechanical speed and β is the pitch angle.

The PMSG mechanical equation is expressed by (4).

$$\frac{d\omega_m}{dt} = \frac{1}{J} (T_{em} - T_m - f \omega_m) \quad (4)$$

where T_{em} is the generated electromagnetic torque (Nm), T_m is the generated turbine mechanical torque (Nm), J the inertia moment (Kgm²) and f is the viscous friction coefficient. The electrical speed of the rotor can be presented as follows

$$\omega = p \omega_m = \frac{p(T_{em} - T_m)}{J_s + f} \quad (5)$$

p represents in this relation the number of pole pairs of the PMSG.

B. PMSG model

In this section, the time continuous PMSG model is presented. The developed model of the generator is developed in the rotating dq reference frame (where d axis is in line with the rotor magnetization axis). The PMSG is modeled by these stator voltage relations [13]

$$\begin{cases} V_{sd} = -\frac{d\Phi_{sd}}{dt} - R_s i_{sd} + \omega \Phi_{sq} \\ V_{sq} = -\frac{d\Phi_{sq}}{dt} - R_s i_{sq} - \omega \Phi_{sd} \end{cases} \quad (6)$$

where R_s is the PMSG stator winding resistance, Φ_{sd} and Φ_{sq} are respectively the d stator flux linkage and the q stator flux linkage. These stator fluxes are expressed according to the following equations

$$\begin{cases} \Phi_{sd} = L_{sd}i_{sd} + \Phi_m \\ \Phi_{sq} = L_{sq}i_{sq} \end{cases} \quad (7)$$

L_{sd} (H) and L_{sq} (H) are the dq -axis self-inductances of the generator.

ϕ_m (Wb) represents here the rotor flux linkage.

The stator currents of the PMSG are computed according to the relation (8), which is deduced from equations (6-7).

$$\begin{cases} i_{sd} = \frac{V_{sd} + \omega L_{sq}i_{sq}}{L_{sd}s + R_s} \\ i_{sq} = \frac{V_{sq} - \omega L_{sd}i_{sd} - \omega\Phi_m}{L_{sq}s + R_s} \end{cases} \quad (8)$$

The PMSG electromagnetic torque is expressed by relation (9)

$$T_{em} = \frac{3p}{2} (\Phi_m i_{sq} + (L_{sd} - L_{sq})i_{sd}i_{sq}) \quad (9)$$

Fig.2 represents the PMSG model developed on MATLAB-Simulink, which is derived from relations (5) to (9).

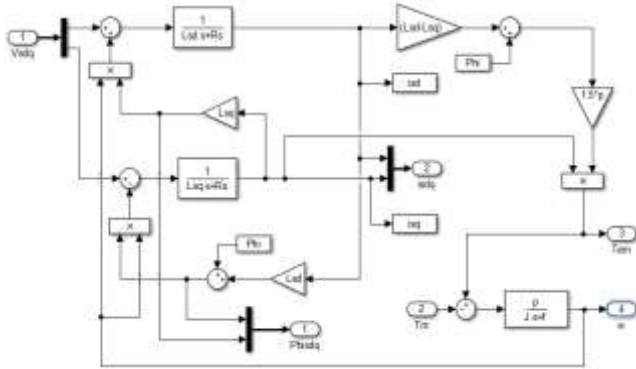


Fig.2.MATLAB-Simulink time-continuous PMSG model

3. Machine Side Converter Model

In this section, the model of the AC-DC converter will be presented. As mentioned previously, the machine-side converter is based on a three-phase diode rectifier and a boost converter. An unregulated DC-link interfaces between the boost converter and the diode rectifier. Fig.3 shows the considered machine side converter.

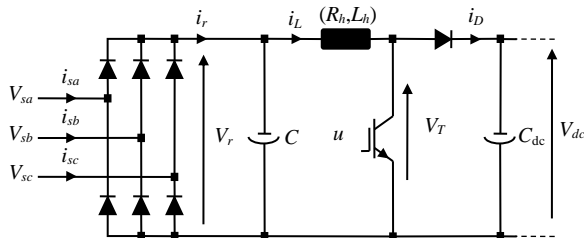


Fig.3.The machine side converter

A. Three-phase diode rectifier associated to an unregulated DC-link Model

The time-continuous model of the diode rectifier is presented in this part. Current can only flow in one direction in an uncontrolled three-phase diode rectifier since it is a one-way device. It is the simplest, most economical, and robust topology used in power electronics. The losses are neglected because the diodes are assumed to be ideal. Rectifier modeling is based on equation (10). In this equation, V_{sk} ($k=(a,b,c)$) refer to the voltages in rectifier AC side, while V_r is the voltage in the DC side. More details on equation (10) can be found in [17].

$$V_{sk} = \frac{V_r}{2} \text{sgn}(i_{sk}) - V_r \frac{[\text{sgn}(i_{sc}) + \text{sgn}(i_{sb}) + \text{sgn}(i_{sa})]}{6} \quad (10)$$

where i_{sa} , i_{sb} , i_{sc} are the currents generated at the stator windings of the PMSG. Finally, k represents the three coefficients a , b and c . The function sgn is equal to

$$\text{sgn}(x) = \begin{cases} 1 & \text{if } x > 0 \\ 0 & \text{if } x = 0 \\ -1 & \text{if } x < 0 \end{cases} \quad (11)$$

As demonstrated by Fig. 4, the voltage V_r across the unregulated DC-link is equal to the voltage in the rectifier DC side. The voltage V_r is computed according to (12).

$$V_r = \frac{1}{C_s} (i_r - i_L) \quad (12)$$

The unregulated DC link is presented by a C capacitor. The current i_L represents the inductance current of the boost converter and the current i_r is the rectifier output current and is given by the relationship below

$$i_r = \gamma_a i_{sa} + \gamma_b i_{sb} + \gamma_c i_{sc} \quad (13)$$

In (13), the function γ is described by (14)

$$\begin{aligned} \gamma_a &= 1 \text{ if } i_{sa} \geq 0 \text{ else } \gamma_a = 0 \\ \gamma_b &= 1 \text{ if } i_{sb} \geq 0 \text{ else } \gamma_b = 0 \\ \gamma_c &= 1 \text{ if } i_{sc} \geq 0 \text{ else } \gamma_c = 0 \end{aligned} \quad (14)$$

B. Boost Converter Model

The used boost converter interfaces between the uncontrolled and controlled DC-links. Its use is for the purpose of controlling the speed of the generator. Here, it should be noted that the voltage of the controlled DC-link will be lower than the voltage of the uncontrolled DC-link. The voltage across the power transistor of the boost converter, noted V_T , depends on the level of the controlled tension V_{dc} and the state of the switching signal u as shown in (15).

$$V_T = (1-u)V_{dc} \quad (15)$$

On the other hand, V_T can be expressed according to (16).

$$V_T = R_h i_L + L_h \frac{di_L}{dt} + V_r \quad (16)$$

which L_h and R_h are respectively the inductance and resistor of the inductive filter used in the boost converter.

Note that when u is equal to 1, the power transistor is conductive while the power diode is blocked, otherwise, when u is equal to 0, the power diode is conductive and the

power transistor is non-conductive. By applying the *Laplace Transform* to the second equation of relation (15), the expression of the current i_L will be deduced according to the following relation

$$i_L = \frac{V_T - V_r}{L_h s + R_h} \tag{17}$$

The output current of the boost converter is denoted i_D as illustrated in Fig.3. This current is computed according to (17).

$$\begin{cases} i_D = (1-u) i_L & \text{if } (1-u) i_L \geq 0 \\ i_D = 0 & \text{if } (1-u) i_L < 0 \end{cases} \tag{18}$$

4. Grid Side Converter Model

A. Controlled DC-Link Model

In this paragraph, the time continuous models of DC-AC converter, regulated DC-link and three-phase inductive filter will be presented. The link between the two conversion stages is the regulated DC-link. The goal of this regulated DC-link is to decouple the electrical power produced by the generator from the electrical energy fed into the grid. In this case, the harmonic content of the stator currents will not assign the quality of the energy fed into the grid [18].

The V_{dc} voltage across the controlled DC-link is described by the following relationship

$$V_{dc} = \frac{1}{C_{dc} s} (i_D - i_{dc}) \tag{19}$$

with i_{dc} is the DC-link output current and C_{dc} is the capacitor of the controlled DC-link.

Based on equation (18), Fig.4 is deduced. This figure represents the Simulink model of the regulated DC-link.

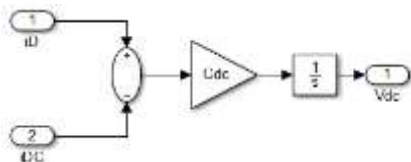


Fig.4.Regulated DC-link model under MATLAB-Simulink

B. Inverter Model

The DC-AC converter supplies the grid with generated power, regulates the amount of active and reactive power and maintains the DC link voltage constant [19]. The output voltage of the inverter is denoted V_{oabc} . It is represented by the following relationship

$$\begin{bmatrix} V_{oa} \\ V_{ob} \\ V_{oc} \end{bmatrix} = \frac{V_{dc}}{3} \begin{bmatrix} 2 & -1 & -1 \\ -1 & 2 & -1 \\ -1 & -1 & 2 \end{bmatrix} \begin{bmatrix} S_a \\ S_b \\ S_c \end{bmatrix} \tag{20}$$

where S_a , S_b and S_c are the switching signals of the DC-AC converter.

Fig.5. shows the Simulink model of the DC-AC inverter.

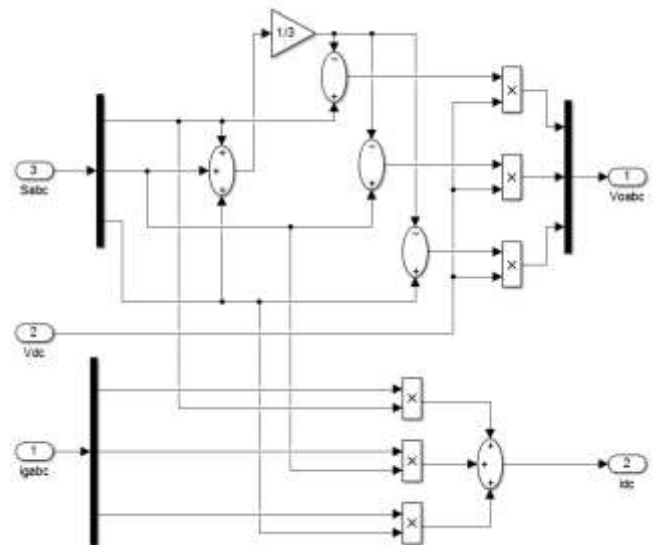


Fig.5.Inverter model under MATLAB-Simulink

C. Inductive filter model

In this part, the time-continuous model of the inductive filter is described. The grid current $i_{g(a,b,c)}$ are deduced according to (20).

$$\begin{bmatrix} i_{ga} \\ i_{gb} \\ i_{gc} \end{bmatrix} = \frac{1}{R_f + L_f s} \left(\begin{bmatrix} V_{ga} \\ V_{gb} \\ V_{gc} \end{bmatrix} - \begin{bmatrix} V_{oa} \\ V_{ob} \\ V_{oc} \end{bmatrix} \right) \tag{21}$$

where $V_{o(a,b,c)}$ represent the voltages at the output inverter and $V_{g(a,b,c)}$ represent the grid voltages components.

The model of the inductive filter is representing in Fig.6.

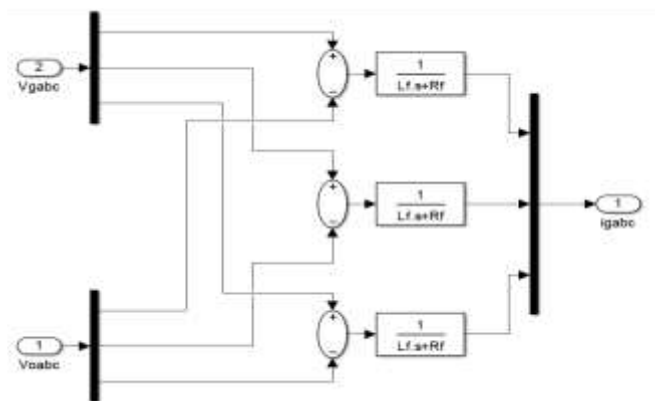


Fig.6. Simulink model of the inductive filter

5. Simulations Results

Simulations results paragraph presents the simulated responses of the considered small wind turbine system. Fig.7 shows the power structure of the small wind turbine system associated by the PMSG along with its controller. The power circuit model is developed under Matlab/Simulink and tested using standard controllers. The control of the generator side converter is consisting of an external speed regulation loop which controls the angular rotational speed ω of the PMSG

and an internal regulation loop that controls the current i_L of the inductor. As regards to the generator side controller, it is also consisting of two regulation parts: An external control loop that controls the V_{dc} voltage level and an internal control loop that controls the injected active and reactive powers to the grid. These controllers are not detailed in this paper and can be found in literature [13]. Tab.1 recaps the system parameters.

For simulation trials, the assumptions presented below are taken into consideration:

- For the generator side control, the speed reference is set to 157 rad.s⁻¹.
- For the grid side control, the reference voltage V_{dc}^* is set equal to 200V.
- The mechanical torque T_m imposed by the turbine, and it is equal to -2Nm.

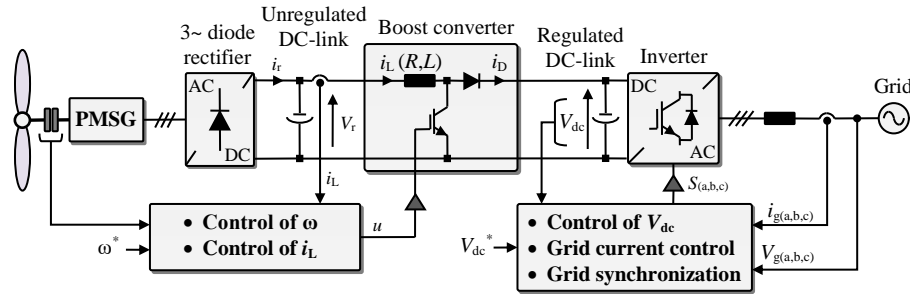


Fig.7. PMSG-based small wind turbine system along with its controller

TABLE I
SYSTEM PARAMETERS

Symbol	Description	value	Unit
PMSG parameters			
p	Pair poles	2	
R_s	Stator resistance	1	Ω
L_{sd}	Auto-inductance on the d axis	0.424	H
L_{sq}	Auto-inductance on the q axis	0.174	H
Φ_r	Rotor flux linkage magnitude	1	Wb
f	Viscous friction coefficient	0.0028	Kg.s ⁻¹
J	Total moment of inertia returned to the motor shaft	0.002	Kg.m ²
Boost converter parameters			
R_h	Inductor internal resistance	0.1	Ω
L_h	Inductor inductance	0.007	H
C	Uncontrolled capacitor	1000	μ F
Inverter parameters			
R	Resistance of the filter	10	Ω
L	Inductance of the filter	0.5	H
Grid parameters			
V_g^{RMS}	Grid voltage RMS value	70	V

Fig.8 to 16 show the simulation results displayed. Fig.8 shows the resulting signal of the voltage V_{sa} applied at the AC side of the diode rectifier on phase a . Fig.9 shows the simulation results for the stator current i_{sa} on phase a , regarding the rectified current i_r measured in the DC side of the diode rectifier. The currents i_{sb} and i_{sc} have the same harmonic contents. It can be noted that, as expected, the stator current is highly distorted ($THD(i_{sa})=12.6\%$) and the i_r current includes a pronounced 6th harmonic component [20-21]. As mentioned previously, this harmonic content will not affect the quality of the power injected to the grid since a DC-link is used to decouple the grid side converter from the generator side converter. The distortion of the PMSG stator currents will also result on notable 6th harmonic ripples in the electromagnetic torque as depicted on Fig.10.

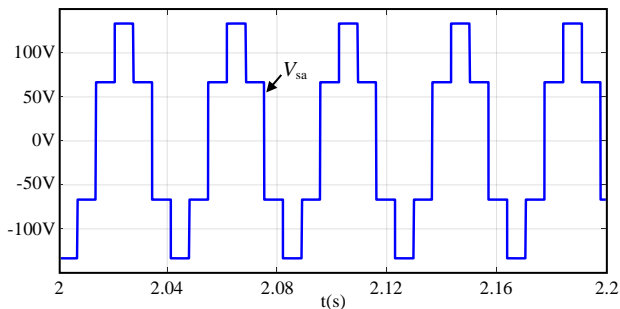


Fig.8. Results of the simulation of the V_{sa} voltage

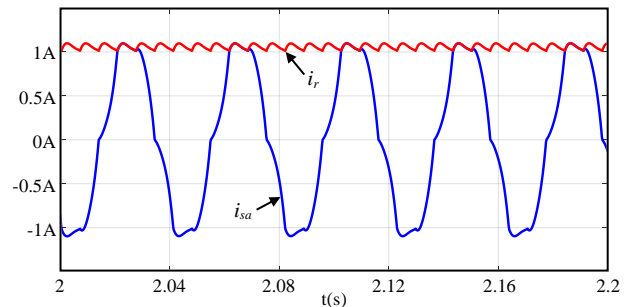


Fig.9.Simulation results of i_{sa} and i_r currents

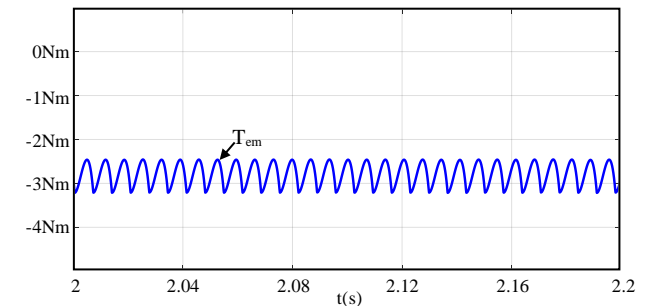


Fig.10.Simulation results T_{em} waveform

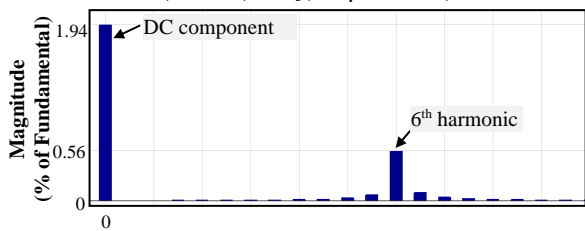


Fig.11.Simulation results FFT of the T_{em}

Fig.12 shows the harmonic spectrum of the electromagnetic torque. A 6th harmonic component is present in the T_{em} signal. Fig.12 and Fig.13 show the simulation results of the PMSG rotational speed ω and the uncontrolled DC-link voltage V_r , respectively. As expected, both signals include 6th harmonic fluctuations which are a natural byproduct of the of a three-phase diode rectifier with non-sinusoidal currents on the AC side.

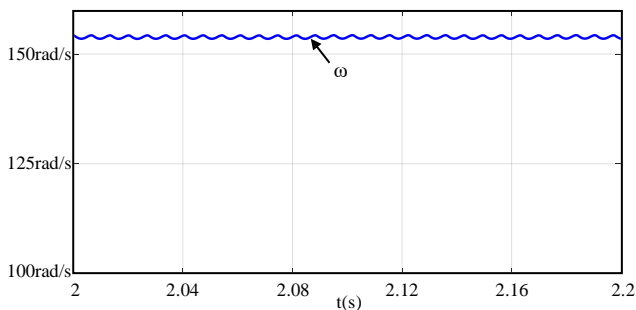


Fig.12. The electrical rotation speed ω signal under MATLAB-Simulink

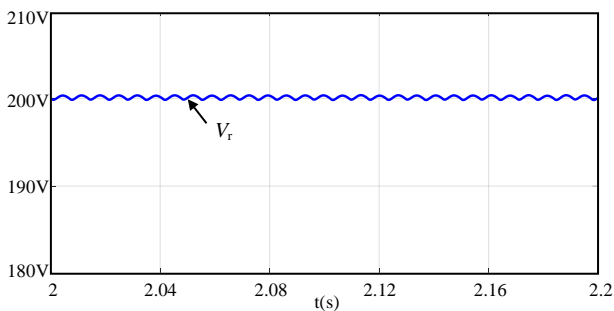


Fig.13. The V_r voltage signal under MATLAB-Simulink

Fig.14 shows the simulation results of the regulated DC-link voltage V_{dc} and of the voltage V_{oa} applied by the three phase DC-AC converter on phase a . The DC-link voltage V_{dc} is well regulated and without low frequency ripples.

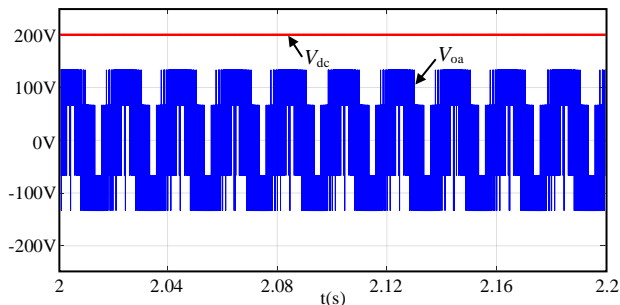


Fig.14. V_{dc} and V_{oa} voltages signals results

Fig.15 shows the simulation results of the grid voltage V_{ga} and the grid current i_{ga} . According to this figure, a unity power factor operation is achieved.

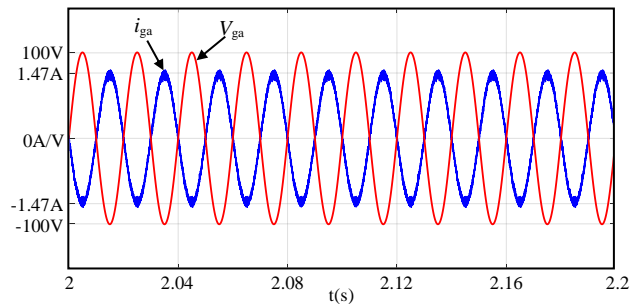


Fig.15. The V_{ga} voltage and i_{ga} current signals results

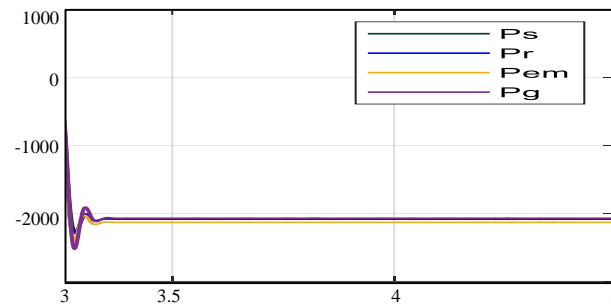


Fig.16. The P_s , P_r , P_{em} and P_g powers signals results

Fig.16 shows the simulation results of the active powers P_s , P_r , P_{em} and P_g . P_{em} represents the electromechanical power injected into the PMSG. P_s represents the active power measured at the output of the PMSG. P_r is the power measured at the output of the three-phase diode rectifier. And P_g is the power injected into the grid. The figure shows that the electromechanical power P_{em} absorbed by the PMSG is fully injected into the grid (P_g) through the entire power conversion chain.

The obtained simulation results confirm the good functionality of the developed models.

6. Conclusion

This work presented a time continuous model for a PMSG-based small wind turbine system. The considered system includes two power conversion stages: an AC-DC converter and a DC-AC converter. The AC to DC power conversion stage is comprised of a rectifier, an uncontrolled DC-link and a boost converter. As regards the second power conversion stage, it composed of a three-phase VSI and an inductive filter. Compared to others research works that are founded on average dynamic models for the modeling of the considered wind turbine system, this paper focused on the development of an accurate time continuous model that considers the nonlinearities introduced by the diode rectifier, the boost converter and the three-phase VSI. The accuracy of the developed model was approved via several simulation tests. The obtained results achieved the interest of the developed model for future work around the control of PMSG-based small wind turbine sources.

Nomenclature

Abbreviations

HAWT: Horizontal Axis Wind Turbines
PMSG: Permanent Magnet Synchronous Generators
RESs: Renewable Energy Sources
VAWT: Vertical Axis Wind Turbines
VSC: Voltage Source Converter
WECS: Wind Energy Conversion Systems
WTSS: Wind Turbine Systems

Parameters

A: the area swept by the rotor blades (m^2)
 C_{dc} is the capacitor of the controlled DC-link
 C_p : the power coefficient represents the ratio of turbine power to the extracted wind power
 f : the viscous friction coefficient
 i_D : the output current of the boost converter
 i_{dc} : the DC-link output current
 $i_{g(a,b,c)}$: the grid current
 i_L : the inductance current of the boost converter
 i_r : the rectifier output current
 i_{sa} , i_{sb} and i_{sc} : the currents generated at the stator windings of the PMSG.
 i_{sdq} : the stator currents of the PMSG
 J : the inertia moment (Kgm^2)
 K : the three coefficients a, b and c.
 L_h : the inductance of the inductive filter used in the boost converter
 L_{sdq} : the dq -axis self-inductances of the generator (H)
 p : the number of pole pairs of the PMSG
 P_{em} : the electromechanical power injected into the PMSG
 P_g : the power injected into the grid.
 P_r : the power measured at the output of the three-phase diode rectifier
 P_s : the active power measured at the output of the PMSG
 $P_{Turbine}$: the output aerodynamic power
 P_{wind} : kinetic power applied to the Wind Turbine
 R_h : the resistor of the inductive filter used in the boost converter
 R_s : the PMSG stator winding resistance
 S_{abc} : the switching signals of the DC-AC converter
 T_{em} : the generated electromagnetic torque (Nm)
 T_m : The wind turbine mechanical torque output
 u : the state of the switching signal
 V_{dc} : the controlled tension
 $V_{g(a,b,c)}$: the grid voltages components
 V_{oabc} : the output voltage of the inverter
 V_r : is the voltage in the DC side
 V_{sdq} : the dq stator voltages
 $V_{sk(k=(a,b,c))}$: the voltages in rectifier AC side
 V_{tr} : the voltage across the power transistor of the boost converter
 V_ω : wind velocity (m/s)
 ω : the angular rotational speed of the PMSG
 ω_m : the rotor mechanical speed (rad/s)
 β : the pitch angle.
 λ : the tip speed ratio

ρ : the density of air (typically 1.225 kg/m³)

ϕ_m : the rotor flux linkage (Wb)

Φ_{sd} : the d stator flux linkage

Φ_{sq} : the q stator flux linkage

Acknowledgements

“This work was supported by the Tunisian Ministry of High Education and Research under Grant LSE-ENITLR11ES15 and funded in part by the Programme d’Encouragement des Jeunes Chercheurs (PEJC) (Code 20PEJC06-08)”

References

- [1] A. Saidi, A. Harrouz, I. Clolak, K. kayisli and Ramazan Bayindir, “Performance Enhancement of Hybrid Solar PV-Wind System Based on Fuzzy Power Management Strategy: A Case Study,” 7th International Conference on Smart Grid, 9-11 December 2019.
- [2] F. Ayadi, I. Colak, I. Garip and H.I. Bulbul, “Targets of Countries in Renewable Energy,” 9th International Conference on Renewable Energy Research and Applications, 27-30 September 2019.
- [3] E. Bekiroglu and M.D. Yazar, “Analysis of Grid Connected Wind Power System,” 8th International Conference on Renewable Energy Research and Applications (ICRERA 2019), 3-6 November 2019.
- [4] A. Harrouz, I. Colak, K. Kayisli, “Energy Modeling Output of Wind System based on Wind Speed,” 8th International Conference on Renewable Energy Research and Applications, 3-6 November 2019.
- [5] N.A. Orlando, M. Liserre, R.A. Mastromauro and A. Dell’Aquila, “A survey of control issues in PMSG-based small wind-turbine systems”, IEEE Trans. Ind. Inf, vol. 9, n°3, pp. 1211–1221, Aug. 2013.
- [6] Y. Xu, H. Nian and L. Chen, “Small-Signal Modeling and Analysis of DC-Link Dynamics in Type-IV Wind Turbine System,” in IEEE Transactions on Industrial Electronics, vol. 68, no. 2, pp. 1423-1433, Feb. 2021.
- [7] D. Cortes-Vega, F. Ornelas-Tellez and J. Anzurez-Marin, “Nonlinear Optimal Control for PMSG-Based Wind Energy Conversion Systems,” in IEEE Latin America Transactions, vol. 19, no. 7, pp. 1191-1198, July 2021.
- [8] S. Vadi, F.B. Gurbuz, R. Bayindir and E. Hossain, “Design and Simulation of a Grid Connected Wind Turbine with Permanent Magnet Synchronous Generator,” 8th IEEE International Conference on Smart Grid, 17-19 June 2020.
- [9] R. Ben Ali, H. Schulte and A. Mami, "Modeling and simulation of a small wind turbine system based on PMSG generator," 2017 Evolving and Adaptive Intelligent Systems, 2017, pp. 1-6.
- [10] A. Harrouz, A. ben Atialah and O. Harrouz, "Modeling of small wind energy based of PMSG in South of Algeria," 2012 2nd International Symposium On Environment Friendly Energies And Applications, 2012.

- [11] S. K. Pillai and P. Samuel, "Dynamic behaviour of UPF rectifier for PMSG based wind energy conversion system," 2014 International Conference on Embedded Systems, 2014, pp. 200-205.
- [12] M. Malinowski, A. Milczarek, R. Kot, Z. Goryca and J. T. Szuster, "Optimized Energy-Conversion Systems for Small Wind Turbines: Renewable energy sources in modern distributed power generation systems," in IEEE Power Electronics Magazine, vol. 2, no. 3, pp. 16-30, Sept. 2015.
- [13] V. Yaramasu and B.Wu, "Model predictive control of wind energy conversion systems," ebook, Wiley, 2017.
- [14] C. Lumbreras, J. M. Guerrero, P. García, F. Briz and D. D. Reigosa, "Control of a Small Wind Turbine in the High Wind Speed Region," in IEEE Transactions on Power Electronics, vol. 31, no. 10, pp. 6980-6991, Oct. 2016.
- [15] M. Rahimi, "Modeling, control and stability analysis of grid connected PMSG based wind turbine assisted with diode rectifier and boost converter," International Journal of Electrical Power & Energy Systems, Vol. 93, pp. 84-93, 2017.
- [16] H. T. Nguyen, A. S. Al-Sumaiti, K. A. Hosani and M. S. E. Moursi, "Multifunctional Control of Wind-Turbine Based Nano-Grid Connected to Distorted Utility-Grid," in IEEE Transactions on Power Systems, vol. 37, no. 1, pp. 576-589, Jan. 2022.
- [17] M. Mansour, M.N. Mansouri and M.F. Mmimouni, "Study and Control of variable-speed WindEnergy System Connected to the Grid," International Journal Of Renewable Energy Research, IJRER, Vol.1, No.2, pp.96-104, 2011.
- [18] P. Pejovic and J. W. Kolar, "Exact Analysis of Three-Phase Rectifiers With Constant Voltage Loads," in IEEE Transactions on Circuits and Systems II: Express Briefs, vol. 55, no. 8, pp. 743-747, Aug. 2008
- [19] M. Karimi-Ghartemani, S. A. Khajehoddin, P. Jain and A. Bakhshai, "A Systematic Approach to DC-Bus Control Design in Single-Phase Grid-Connected Renewable Converters," in IEEE Transactions on Power Electronics, vol. 28, no. 7, pp. 3158-3166, July 2013.
- [20] Yazdani, Amirnaser, and R. Iravani, "Voltage-sourced converters in power systems: modeling, control, and applications". Ebook, Wiley, 2010.
- [21] A. Belkaid, I. Colak, K. Kagisli and R. Bayindir, "Modeling of Permaenet Magnet Synchronous Generator in a Power Wind Generation System with an Electrochemical Energy Storage", International Journal of Smat Grid, Vol.2, No.4, December 2018.